PHYSICAL REVIEW LETTERS

# Quantifying Water Density Fluctuations and Compressibility of Hydration Shells of Hydrophobic Solutes and Proteins

Sapna Sarupria and Shekhar Garde*

*The Howard P. Isermann Department of Chemical & Biological Engineering,
and Center for Biotechnology and Interdisciplinary Studies, Rensselaer Polytechnic Institute,
110 8th Street, Troy, New York 12180, USA*

We probe the effects of solute length scale, attractions, and hydrostatic pressure on hydrophobic hydration shells using extensive molecular simulations. The hydration shell compressibility and water fluctuations both display a nonmonotonic dependence on solute size, with a minimum near molecular solutes and enhanced fluctuations for larger ones. These results and calculations on proteins suggest that the hydration shells of unfolded proteins are more compressible than of folded ones contributing to pressure denaturation. More importantly, the nonmonotonicity implies a solute curvature-dependent pressure sensitivity for interactions between hydrophobic solutes.

Hydrophobicity has emerged as a multidimensional challenge in the space of thermodynamic conditions [1–6] and parameters such as solute length scale [7,8] and solute-water attractions [9,10]. Idealized hydrophobes, hard spheres, dewet with increasing size, and the corresponding crossover in their hydration thermodynamics and structure is known [1,7,11,12]. Solute-water attractions wet the solute surface [9,10] and, in turn, affect water-mediated solute-solute interactions [10,13]. The (de)wetting characterizes changes only in the one-particle inhomogeneous density of vicinal water. Higher-order correlations, and correspondingly local density fluctuations, will also be affected by solute length scale and attractions. These fluctuations provide a direct measure of the hydration shell compressibility and characterize how the local density responds to pressure [14]. That response is intimately connected to how pressure affects conformations of macromolecular solutes, especially proteins.

Here we use extensive molecular dynamics (MD) simulations to quantify density fluctuations in and compressibility of hydrophobic hydration shells over a range of solute sizes (~0.1–2 nm), hydrostatic pressures (1—4000 bar), and solute-water attractions. We show that the hydration shell compressibility varies nonmonotonically with solute size, displaying a minimum for molecular solutes and increasing significantly for larger ones. Although attractions increase the hydration shell density and suppress density fluctuations, the nonmonotonic variation of compressibility with solute size persists for attractive solutes. We discuss the origins of nonmonotonicity and show that the enhanced fluctuations near larger solutes distinguish the hydration shell from bulk water. We also discuss the implications of enhanced fluctuations on pressure effects on proteins.

Figure 1(a) shows solute-water oxygen radial distribution functions (RDFs) for Weeks-Chandler-Anderson

(WCA) solutes. The smallest solute perturbs its environment negligibly, and the vicinal density is close to that in bulk [also see Fig. 2(b)]. Near slightly larger solutes ($R^* \sim$ 0.3–0.4 nm), water packs well showing a layered structure with clearly defined hydration shells. Further increase in solute size causes a gradual dewetting reflected in lowering of the first peak [Fig. 1(b)] and of average hydration shell density at 1 bar [Fig. 2(b)]. How does the hydration shell water respond to pressure? With increasing pressure, the solute-water RDFs become better defined for all solutes,
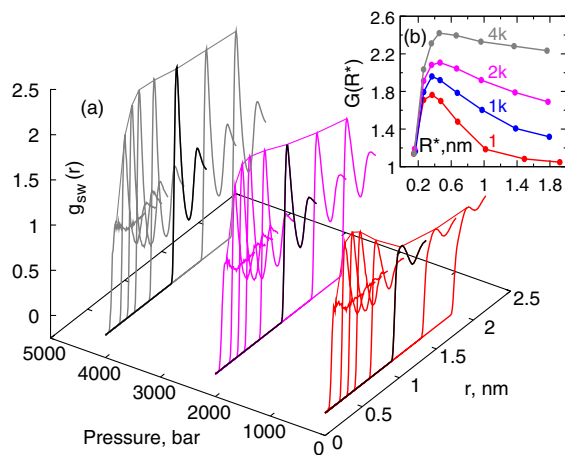


FIG. 1 (color online). (a) Solute-water RDFs for a range of solute sizes and pressures at 300 K. The black curve is for a solute with a radius of ~1 nm. (b) The height of the first peak near different solutes. $R^*$ is the peak location. Data are from simulations of 8 WCA [27] solutes in SPC/E [28] water in the ($N$, $P$, $T$) ensemble. The WCA potential for a Lennard-Jones methane ($\sigma_{sw} = 0.345$ nm and $\epsilon_{sw} = 0.8957$ kJ/mol) was shifted horizontally by $-0.25$, $-0.1$, $0.0$, $0.1$, $0.3$, $0.6$, $1.0$, and $1.4$ nm to represent 8 WCA solutes. Simulations included one solute and 1100—7250 waters depending on the solute size.
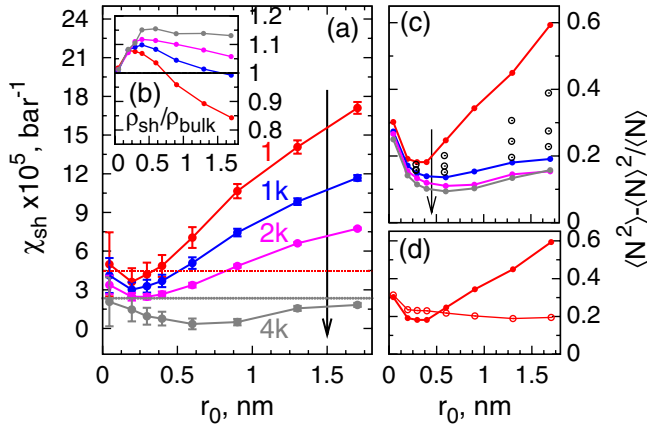
FIG. 2 (color online). (a) Hydration shell compressibility. Hydration shell is defined using solute-water RDF at 1 bar. The inner radius $r_0$, such that $-\ln[g_{sw}(r_0)] = 5$, quantifies the solute cavity radius. The outer radius is the location of the first minimum in $g_{sw}(r)$. (b) Average hydration shell density normalized by the bulk value. (c) Normalized water number fluctuations in the shell. Open symbols in (c) are data at 250, 500, and 750 bar. (d) The same as in (c) for 1 bar. Open symbols in (d) are fluctuations in hydration-shell-shaped volumes centered at an arbitrary point in bulk water.

but especially for the larger ones [Fig. 1(a)], and the height of the first peak increases [Fig. 1(b)], indicating a positive local compressibility. We obtained the hydration shell compressibility $\chi_{sh} = (1/\rho_{sh})[\partial\rho_{sh}/\partial P]_T$ as a function of solute size at different pressures [Fig. 2(a)]. At 1 bar, $\chi_{sh}$ varies nonmonotonically with solute size. Smallest solutes cause minor perturbations to vicinal water, and the local compressibility is bulklike. With increasing solute size, compressibility goes through a minimum, before increasing to about 4 times the bulk value near nanometer-sized and larger solutes. Pressure squeezes water molecules into the hydration shell, gradually decreasing the ability to further accept water molecules, decreasing $\chi_{sh}$ for all solutes, but especially for the larger ones. Nevertheless, the nonmonotonic variation of $\chi_{sh}$ with solute size is observed at all pressures studied here. Also, with increasing pressure, the location of the minimum shifts to the right and is in the 0.5–1 nm size range at 4000 bar.

Do hydration shell fluctuations track the behavior of isothermal compressibility shown above? In the thermodynamic ($N \to \infty$) limit, for a grand-canonical system, isothermal compressibility is related to particle number fluctuations in the system volume $V$ as $\chi = \frac{\langle N^2\rangle - \langle N\rangle^2}{\langle N\rangle^2}\frac{V}{kT}$. Figure 2(c) shows normalized hydration shell water number fluctuations as a function of solute size and hydrostatic pressure. Indeed, the fluctuations display a nonmonotonic variation with solute size similar to that of compressibility in Fig. 2(a). With increasing pressure, the fluctuations are suppressed, with most significant change occurring over the 1–1000 bar window. What is the origin of the minimum in $\chi_{sh}$? In the $V \to 0$ limit, the scaled particle theory (SPT)

[15] gives $p(0) = 1 - \rho V$ and $p(1) = \rho V$, where $p(i)$ is the probability of observing $i$ particles in volume $V$. Thus, for small volumes, normalized fluctuations will decrease with increasing volume (with slope $-\rho$): $(\langle N^2\rangle - \langle N\rangle^2)/\langle N\rangle = 1 - \rho V$, which is indeed observed in the hydration shell as well as in similarly shaped volumes in bulk water. In fact, in bulk water, the normalized fluctuations decrease and asymptotically approach a limiting value expected from bulk compressibility [Fig. 2(d)]. In hydration shells, near $V = 0$, increasing pressure decreases fluctuations at a faster rate as expected from the SPT [Fig. 2(c)]. Near larger solutes, however, vicinal water correlations are affected, and the fluctuations are enhanced, a behavior that is distinct from that in the bulk. Bratko *et al.* [16] have reported enhanced fluctuations for water confined between hydrophobic plates, which are suppressed by pressure. Mittal and Hummer [17] also observed enhancement of fluctuations with increasing solute size. Because their smallest solute lies close to the location of our compressibility minimum and they explore the negative pressure range, they do not observe the nonmonotonic behavior of fluctuations.

How does the presence of a solute affect water-water correlations in its hydration shell? The two-particle correlation conditioned on the presence of the solute, $\rho^{(2)}(\mathbf{r_1}, \mathbf{r_2}|\mathbf{r_S})$, is related to lower order correlations by $\rho^{(2)}(\mathbf{r_1}, \mathbf{r_2}|\mathbf{r_S}) = \rho^{(1)}(\mathbf{r_1}|\mathbf{r_S})\rho^{(1)}(\mathbf{r_2}|\mathbf{r_S})g^{(2)}(\mathbf{r_1}, \mathbf{r_2}|\mathbf{r_S})$, where $\rho^{(1)}(\mathbf{r}|\mathbf{r_S}) = \rho_b g_{sw}(r)$. For hydration shell water, we approximate $g^{(2)}(\mathbf{r_1}, \mathbf{r_2}|\mathbf{r_S}) \approx g_{ww}^{sh}(r)$. Thus, $\rho^{(2)}(\mathbf{r_1}, \mathbf{r_2}|\mathbf{r_S}) \approx \rho_b^2 g_{sw}(r_1)g_{sw}(r_2)g_{ww}^{sh}(r)$. We obtain $g_{ww}^{sh}(r)$ by normalizing the frequency of observing two hydration shell water oxygens in a given separation window by the frequency of an ideal gas particle pair in that window. We generated positions of ideal gas particles separately in the hydration shell
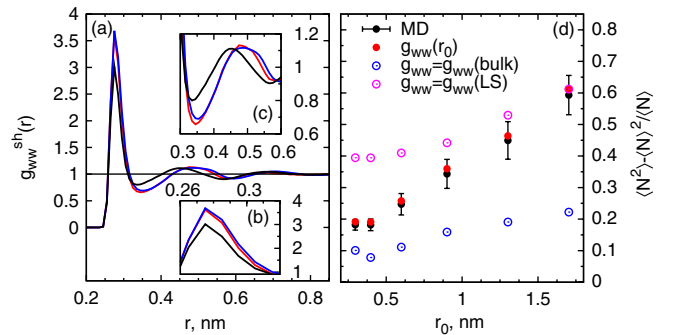


FIG. 3 (color online). (a) Water-water pair correlations $g_{ww}^{sh}(r)$ at 1 bar, in the hydration shell of small ($r_0 \sim 0.3$ nm, red) and large ($r_0 \sim 1.7$ nm, blue) solutes. Bulk water RDF (black) is also shown. Panels (b) and (c) zoom into two regions of interest. (d) Normalized fluctuations measured from MD simulations compared to predictions of compressibility equation using different $g_{ww}^{sh}(r)$: measured $g_{ww}^{sh}$ (red); $g_{ww}^{sh} \approx g_{ww}^{bulk}$ (blue); and $g_{ww}^{sh}$ from the shell of the largest solute (LS) (magenta).

volume for each solute, such that the solute-ideal gas RDF is identical to the solute-water RDF.

Figure 3(a) shows $g_{ww}^{sh}(r)$ profiles in the hydration shell of a small and a large solute, which are subtly different from each other and different from bulk RDF. Specifically, relative to bulk RDF, (i) the short range features, including the first and second peaks and the first minimum, are somewhat enhanced, and (ii) the locations of the first minimum, the second peak, and subsequent features are moved outwards by ~0.05 nm, possibly suggesting an increase in the range of correlations in the solute vicinity. Experimental data for water correlations in hydration shells are not available. Simulations of water at the alkane-water liquid-liquid or water vapor-liquid (V-L) interface or water under tension suggest a similar enhancement of RDF peaks [18,19]. A large correlation length at V-L interface is well known [20,21]. The soft, fluctuating, V-L-like picture of a large hydrophobic solute-water interface [17] is consistent with the correlation length being higher than in bulk. The finiteness of the hydration shell, however, puts a clear upper bound on that length. Thus, it is interesting that water correlations in the hydration shell are subtly different from those in the bulk and display characteristics of water in low density or interfacial environments.

The compressibility equation relates water correlations $g_{ww}^{sh}(r)$ to the hydration shell fluctuations:

$$[\langle N^2 \rangle - \langle N \rangle^2]/\langle N \rangle = 1 + 1/\rho v \times \int_v \int_v [\rho^{(2)}(\mathbf{r_1}, \mathbf{r_2}|\mathbf{r_s})$$
$$- \rho^{(1)}(\mathbf{r_1}|\mathbf{r_s})\rho^{(1)}(\mathbf{r_2}|\mathbf{r_s})]d\mathbf{r_1}d\mathbf{r_2}.$$

Figure 3(b) shows that water number fluctuations predicted by the above equation using $\rho^{(2)}(\mathbf{r_1}, \mathbf{r_2}|\mathbf{r_S}) \approx \rho_b^2 g_{sw}(r_1)g_{sw}(r_2)g_{ww}^{sh}(r)$ with $g_{ww}^{sh}(r)$ measured for each solute are in quantitative agreement with values from MD simulations. In contrast, using $g_{ww}^{sh}(r)$ obtained either near a large solute or in bulk water as $g_{ww}^{sh}(r)$ for all solutes predicts the solute-size dependence of fluctuations poorly, indicating that subtle changes in the inhomogeneous two-particle correlations are indeed important.

Figure 4 shows the effects of solute-water attractions on hydration shell structure and fluctuations. Figures 4(a)–4(c) collectively show that adding attractions increases local water density, with the effect being more prominent for larger solutes. Further, for all solutes, and especially for the larger ones, the compressibility decreases and fluctuations are correspondingly suppressed with increasing attractions. Suppression of fluctuations with external electric fields [22] or near charged side chains of proteins [23] is known. For attractive hydrophobic solutes, we note that both the hydration shell compressibility and fluctuations display a nonmonotonic variation with solute size over a range of attractions, indicating that the trends observed here are not limited to idealized hydrophobic solutes.
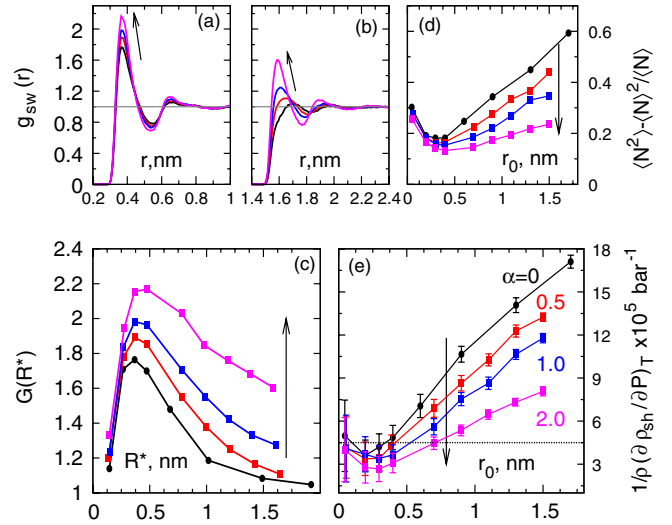


FIG. 4 (color online). Effects of solute-water attractions on solute-water RDFs [(a),(b)], on $G(R^*)$ [(c)], on fluctuations [(d)], and on hydration shell compressibility [(e)]. Panels (a) and (b) are for a methane-sized and for a larger solute with $r_o \sim 1.5$ nm, respectively. To add attractions, the WCA part for a methane-sized solute is shifted down by $\alpha\epsilon$ and connected smoothly to the attractive part $\alpha u_{LJ}(r)$ at the minimum. This potential is shifted horizontally (as in Fig. 1) to study 8 different solutes. Four values of $\alpha$ are shown: 0.0 (WCA, black), 0.5 (red), 1.0 (blue), and 2.0 (magenta).

Experiments show that many globular proteins unfold reversibly at pressures of several kilobars [24]. Correspondingly, the partial molar volume of unfolded states is lower than of folded ones [24]. How hydration shells respond to pressure makes an important contribution to the volume change but is difficult to isolate from experimental data. Dadarlat and Post [23] show that hydration shell compressibilities near protein side chains decrease with increasing attractions, as in hydrophobic > polar > charged groups, as also seen in our results. Thus, hydration shells of unfolded states with their larger exposure of hydrophobic residues will be more compressible. To test this, we performed MD simulations of the protein staph nuclease in folded and unfolded states over a range of pressures [25]. Figure 5 shows that normalized hydration shell fluctuations are indeed higher for unfolded states at all pressures. Also, the difference in fluctuations near folded and unfolded states reduces with increasing pressure, consistent with the suppression of fluctuations by pressure observed above.

The higher hydration shell compressibility near hydrophobic solutes implies that hydrophobic interactions will, in general, weaken with increasing pressure, consistent with the predictions of Hummer et al. [6]. More importantly, the nonmonotonic variation of compressibility with solute size implies a curvature-dependent pressure sensitivity of hydrophobic interactions, not anticipated by those previous studies. We predict that hydrophobic contacts of
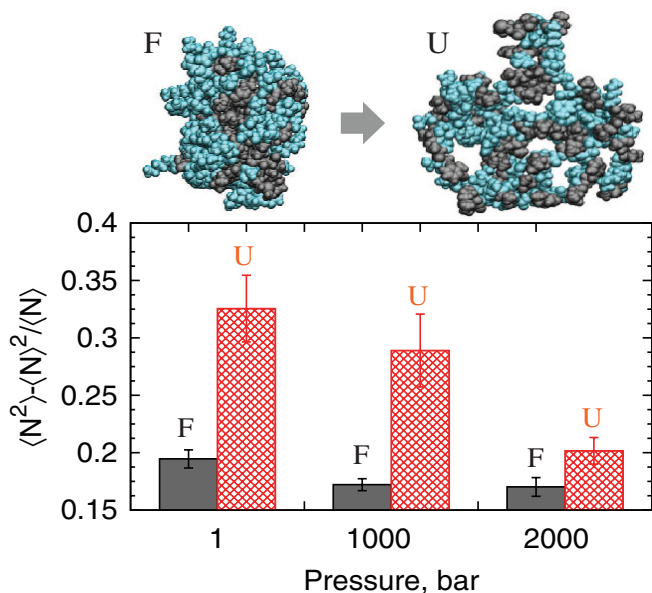
FIG. 5 (color online).   Water number fluctuations in hydration shells of folded (F) and unfolded (U) states of staph nuclease (pdb-id: 1EY0) at different pressures. Unfolded states were generated using a water insertion algorithm [25]. Hydration shell waters are within 0.5 nm of protein. Data are from MD simulations of one protein solvated in 10 684 SPC/E water molecules in the $(N, P, T)$ ensemble. Snapshots of folded and unfolded configurations are shown: hydrophobic residues (gray), others (blue), and water (not shown).

low curvature surfaces would be more pressure sensitive. This principle is also likely at work in the pressure dissociation of multimeric protein complexes or of protein aggregates in inclusion bodies [26].

   We have shown that hydration shell fluctuations and compressibility display a nonmonotonic dependence on the size of hydrophobic solutes. The suppression of fluctuations with increasing attractions suggests that the extent of fluctuations may serve as a sensitive measure of hydrophobicity or -philicity. Fluctuations in shells of hydrophobic residues can contribute significantly to protein hydration shell compressibility thereby affecting their pressure sensitivity. How it manipulates protein stability and interactions quantitatively presents an important future direction to pursue.

*To whom all correspondence should be addressed.
gardes@rpi.edu; http://www.rpi.edu/~gardes
[1] D. Chandler, Nature (London) **437**, 640 (2005).
[2] L. R. Pratt, Annu. Rev. Phys. Chem. **53**, 409 (2002).
[3] R. Zangi *et al.*, J. Am. Chem. Soc. **129**, 4678 (2007).
[4] H. S. Ashbaugh *et al.*, J. Chem. Phys. **116**, 2907 (2002).
[5] S. Garde *et al.*, Phys. Rev. Lett. **77**, 4966 (1996).
[6] G. Hummer *et al.*, Proc. Natl. Acad. Sci. U.S.A. **95**, 1552 (1998).
[7] K. Lum *et al.*, J. Phys. Chem. B **103**, 4570 (1999).
[8] H. S. Ashbaugh and L. R. Pratt, Rev. Mod. Phys. **78**, 159 (2006).
[9] L. Maibaum and D. Chandler, J. Phys. Chem. B **111**, 9025 (2007).
[10] N. Choudhury and B. M. Pettitt, J. Am. Chem. Soc. **129**, 4847 (2007).
[11] F. H. Stillinger, J. Solution Chem. **2**, 141 (1973).
[12] S. Rajamani, T. M. Truskett, and S. Garde, Proc. Natl. Acad. Sci. U.S.A. **102**, 9475 (2005).
[13] X. Huang, C. J. Margulis, and B. J. Berne, Proc. Natl. Acad. Sci. U.S.A. **100**, 11 953 (2003).
[14] N. Giovambattista *et al.*, Phys. Rev. E **73**, 041604 (2006).
[15] H. Reiss, Adv. Chem. Phys. **9**, 1 (1965).
[16] D. Bratko *et al.*, J. Chem. Phys. **115**, 3873 (2001).
[17] J. Mittal and G. Hummer, Proc. Natl. Acad. Sci. U.S.A. **105**, 20 130 (2008).
[18] I. Omelyan *et al.*, Chem. Phys. Lett. **397**, 368 (2004).
[19] M. E. Parker and D. M. Heyes, J. Chem. Phys. **108**, 9039 (1998).
[20] F. P. Buff *et al.*, Phys. Rev. Lett. **15**, 621 (1965).
[21] J. D. Weeks, J. Chem. Phys. **67**, 3106 (1977).
[22] D. Bratko *et al.*, Faraday Discuss. **141**, 55 (2009).
[23] V. Dadarlat and C. Post, Biophys. J. **91**, 4544 (2006).
[24] C. A. Royer, Biochim. Biophys. Acta **1595**, 201 (2002).
[25] S. Sarupria *et al.* (unpublished).
[26] Y. S. Kim *et al.*, in *Amyloid, Prions, and Other Protein Aggregates*, Part C, Methods in Enzymology Vol. 413 (Academic Press, San Diego, 2006), pp. 237–253.
[27] J. D. Weeks, D. Chandler, and H. C. Andersen, J. Chem. Phys. **54**, 5237 (1971).
[28] H. J. C. Berendsen *et al.*, J. Phys. Chem. **91**, 6269 (1987).